inter.noise 2000
The 29th International Congress and Exhibition on Noise Control Engineering
27-30 August 2000, Nice, FRANCE

I-INCE Classification: 7.6

AN EFFICIENT PREDICTION TECHNIQUE FOR THE STEADY-STATE DYNAMIC ANALYSIS OF FLAT PLATES

B. Van Hal, W. Desmet, D. Vandepitte, P. Sas

Katholieke Universiteit Leuven, Celestijnenlaan 300B, 3001, Heverlee, Belgium

Tel.: +32 16 32 2523 / Fax: +32 16 32 2987 / Email: bas.vanhal@mech.kuleuven.ac.be

Keywords:
PREDICTION TECHNIQUE, DYNAMIC PLATE PROBLEMS, COMPUTATIONAL EFFICIENCY

ABSTRACT
The finite element (FE) method is the most commonly used prediction technique for solving time-harmonic plate problems. Since the dynamic variables within the plate domain are expanded in terms of simple, approximating shape functions, a large amount of elements is required to get a reasonable prediction accuracy and this amount increases with frequency. This may result in large, computationally expensive models, so that the use of FE models is practically restricted to low-frequency predictions. A newly developed technique, which is based on the indirect Trefftz method, uses wave functions, which are exact solutions of the governing partial differential equations, to expand the dynamic variables. The contributions of the wave functions to the field variable solutions are obtained from a weighted residual formulation of the boundary conditions. Since an approximation is only involved with the boundary conditions, the main asset of this method, compared with the FE method, is the small size of the resulting prediction model. The major drawbacks of the method is that the prediction model becomes fully populated and frequency-dependent. This paper compares the performance of the new prediction technique with conventional FE models for several convex plates with a mixture of various types of boundary conditions. These examples illustrates that the new technique provides a high (displacement and stress) prediction accuracy with smaller computational efforts. In this way, the Trefftz-based prediction technique can be applied up to much higher frequencies, allowing accurate deterministic predictions for the mid-frequency range.

1 - INTRODUCTION

The finite element (FE) method is practically restricted to low-frequency dynamic simulations due to its large computational load. Especially for coupled vibro-acoustic problems, for which FE models are no longer symmetric, the method involves huge computational efforts. Recently, a new wave based (WB) prediction technique for coupled problems has been developed, which exhibits an enhanced computational efficiency, compared to the FE method. This paper illustrates that even for uncoupled plate problems, for which the FE method yields efficient symmetric models, a proper numerical implementation of the WB technique results also in a computationally more efficient technique than the FE method.

2 - BASIC CONCEPTS OF THE PREDICTION TECHNIQUE

2.1 - Problem definition

The differential equation, describing the steady-state out-of-plane displacement response $w(\vec{r}) \cdot e^{j\omega t}$ of a flat plate due to a time-harmonic normal point force excitation $F \cdot e^{j\omega t}$ (see figure 1), is

$$\left(\Delta^2 - k_b^4\right) \cdot w(\vec{r}) = \frac{F}{D} \delta\left(\vec{r} - \vec{r}_F\right) \text{ in } \Omega \tag{1}$$

where $\Delta = \frac{\partial^2}{\partial x^2} + \frac{\partial^2}{\partial y^2}$ represents the Laplace operator, $k_b = \sqrt{\frac{\rho^2}{D}}$ the plate bending wave number, $D = \frac{Et^3(1+j\eta)}{12(1-\nu^2)}$ the plate bending stiffness with plate thickness t, circular frequency ω, material density ρ, Young's modulus E, structural damping factor η and Poisson constant ν.

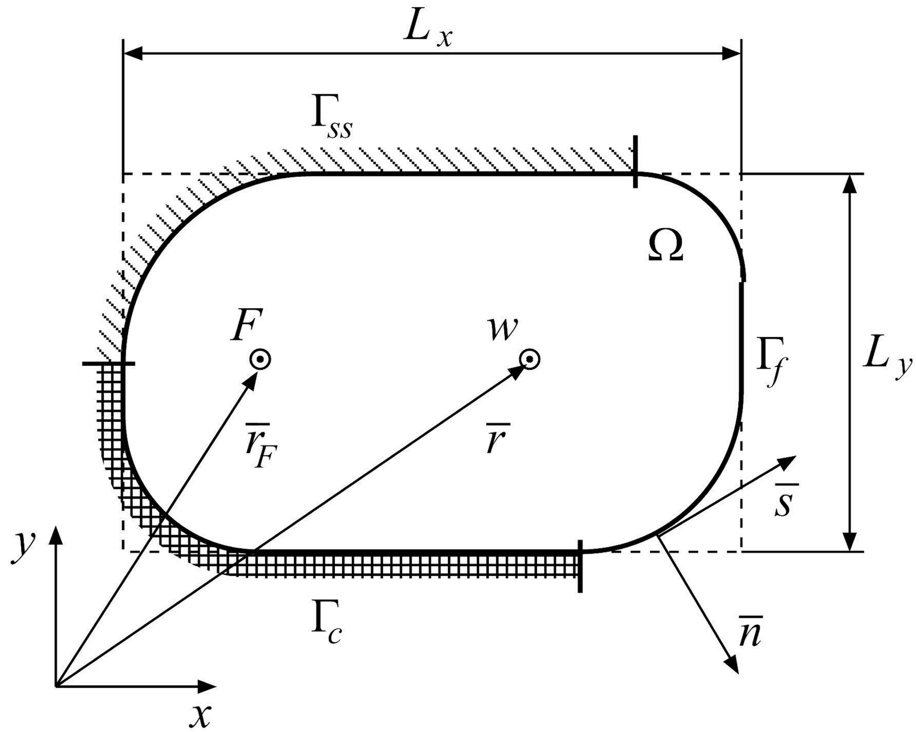

Figure 1: Problem definition.

Three different types of boundary conditions (BC's) are considered, namely
1) clamped BC's at boundary Γ_c:

$$w = 0,\ L_\vartheta (w) = 0 \tag{2}$$

2) simply supported BC's at boundary Γ_{ss}:

$$w = 0,\ L_m (w) = 0 \tag{3}$$

3) free BC's at boundary Γ_f:

$$L_m (w) = 0,\ L_Q (w) = 0 \tag{4}$$

where the linear operators L_* are defined as follows

$$L_\vartheta = -\frac{\partial}{\partial n} \tag{5}$$

$$L_m = -D \left(\frac{\partial^2}{\partial n^2} + \nu \frac{\partial^2}{\partial s^2} \right) \tag{6}$$

$$L_Q = -D \frac{\partial}{\partial n} \left(\frac{\partial^2}{\partial n^2} + (2 - \nu) \frac{\partial^2}{\partial s^2} \right) \tag{7}$$

where $\dfrac{\partial}{\partial n}$ and $\dfrac{\partial}{\partial s}$ are the derivatives with respect to the normal direction $\vec{n}$ and the tangential direction $\vec{s}$ of the plate boundary, respectively.

2.2 - Response approximation
The deterministic WB technique [1], which is based on the indirect Trefftz approach [2], approximates $w(\vec{r})$ as a linear combination of wave functions $\Psi_i(\vec{r})$, extended with a particular solution function $w_F(\vec{r} - \vec{r}_F)$,

$$w(\vec{r}) \approx \hat{w}(\vec{r}) = \sum_{i=1}^{n} w_i \Psi_i (\vec{r}) + w_F (\vec{r} - \vec{r}_F) \tag{8}$$

with

$$\Psi_i(\vec{r}) = \Psi_i(x,y) = e^{-j(k_{x,i}x + k_{y,i}y)} \tag{9}$$

and

$$\left(k_{x,i}^2 + k_{y,i}^2\right)^2 = k_b^4 \tag{10}$$

where n is the number of wave functions, and where w_i are the unknown wave function contribution factors. The response of an infinite plate to a normal point force excitation is selected as particular solution function,

$$w_F(\vec{r} - \vec{r}_F) = \frac{-jF}{8k_b^2 D}\left(H_0^{(2)}(k_b \|\vec{r} - \vec{r}_F\|) - H_0^{(2)}(-jk_b \|\vec{r} - \vec{r}_F\|)\right) \tag{11}$$

where $H_0^{(2)}$ represents the zero-order Hankel function of the second kind.

2.3 - Weighted residual formulation

The approximation $\hat{w}(\vec{r})$ exactly satisfies the plate equation (1), irrespective of the values of the unknown wave function contribution factors w_i. These factors are merely determined by the BC's. The residual error functions along the boundaries are

$$R_w = \hat{w} \text{ on } \Gamma_c \cup \Gamma_{ss} \tag{12}$$

$$R_\vartheta = L_\vartheta(\hat{w}) \;\text{ on } \Gamma_c \tag{13}$$

$$R_m = L_m(\hat{w}) \;\text{ on } \Gamma_{ss} \cup \Gamma_f \tag{14}$$

$$R_Q = L_Q(\hat{w}) \;\text{ on } \Gamma_f \tag{15}$$

$$R_{cw} = \hat{w} \text{ on } n_w \text{ corner points of } \Gamma_c \cup \Gamma_{ss} \tag{16}$$

$$R_{cF} = L_F(\hat{w}) \;\text{ on } n_F \text{ corner points of } \Gamma_f \tag{17}$$

with

$$L_F = -D(1-\nu)\left(\frac{\partial^2}{\partial n^+ \partial s^+} - \frac{\partial^2}{\partial n^- \partial s^-}\right) \tag{18}$$

where the corner points are those boundary points for which the normal vector $\vec{n}$ is not uniquely defined. The directions $\vec{n}^+$ and $\vec{n}^-$ in (18) are the normal directions of the two boundary sections to which the corner point belongs. The residual error functions R_{cw} and R_{cF} are included for reasons of model symmetry. By weighing the residuals with functions, obtained from applying the linear operators L_* to a weighting function $\tilde{w}(\vec{r})$, the weighted residual formulation of the BC's becomes

$$\begin{gathered}\int_{\Gamma_c \cup \Gamma_{ss}} L_Q(\tilde{w}) \cdot R_w d\Gamma + \int_{\Gamma_c} L_m(\tilde{w}) \cdot R_\vartheta d\Gamma - \int_{\Gamma_{ss} \cup \Gamma_f} L_\vartheta(\tilde{w}) \cdot R_m d\Gamma \\ - \int_{\Gamma_f} \tilde{w} \cdot R_Q d\Gamma + \sum_{c=1}^{n_w} L_F(\tilde{w}) \cdot R_{cw} - \sum_{c=1}^{n_F} \tilde{w} \cdot R_{cF} = 0\end{gathered} \tag{19}$$

Using each wave function $\Psi_i(\vec{r})$ in (8) as a weighting function $\tilde{w}(\vec{r})$ in (19) results in a symmetric, frequency-dependent wave model

$$\mathbf{A} \cdot \mathbf{w} = \mathbf{f} \tag{20}$$

where vector $\mathbf{w}$ contains the unknown wave function contribution factors w_i.

2.4 - Wave function selection

The following complete set of wave functions is proposed [1]

$$\Psi_i(x,y) = \begin{cases} \cos(k_{x,p}x) \cdot e^{-j(k_{y,p}y)} \\ e^{-j(k_{x,q}x)} \cdot \cos(k_{y,q}y) \end{cases} \tag{21}$$

with

$$\begin{aligned} k_{x,p} &= \frac{p\pi}{L_x},\ k_{y,p} = \begin{cases} \pm\sqrt{k_b^2 - k_{x,p}^2} \\ \pm j\sqrt{k_b^2 + k_{x,p}^2} \end{cases} \quad , \ p = 0,1,\ldots,n_p \\ k_{y,q} &= \frac{q\pi}{L_y},\ k_{x,q} = \begin{cases} \pm\sqrt{k_b^2 - k_{y,q}^2} \\ \pm j\sqrt{k_b^2 + k_{y,q}^2} \end{cases} \quad , \ q = 0,1,\ldots,n_q \end{aligned} \tag{22}$$

where L_x and L_y represent the dimensions of the smallest enclosing rectangle of the plate domain Ω (see figure 1). Desmet [1] proves that a sufficient condition for the wave function selection (21) to converge towards the exact solution is that Ω is convex. A non-convex Ω requires a division into convex subdomains. In a numerical implementation the complete set (22) is truncated at finite values n_p and n_q,

$$n_p \geq \frac{k_b L_x}{\pi} + 1 \qquad \text{and} \qquad n_q \geq \frac{k_b L_y}{\pi} + 1 \tag{23}$$

such that the plate bending wavelength $\lambda_b = 2\pi/k_b$ is not smaller than the smallest wavelength $\lambda = 2\pi/k$ in the truncated wave function set.

2.5 - Numerical integration

The construction of the wave model (20) involves the evaluation of complex integrals, which are numerically approximated with a Gauss quadrature rule. For increasing wave numbers $k_{x,p}$ and $k_{y,q}$, the complex integration functions in (19) exhibit an increasing spatially oscillating nature. Because the largest values of $k_{x,p}$ and $k_{y,q}$ depend on k_b (see (23)), the number of Gauss points n_{gp} is related to k_b,

$$n_{gp} \geq \max(2k_b, n_{gp,0}) \tag{24}$$

where $n_{gp,0}$ represents an arbitrary minimal number of Gauss points.

3 - NUMERICAL VALIDATION EXAMPLE

A convex aluminum plate of 1mm thickness is considered, as shown in figure 2(a). Part of the plate boundary has clamped BC's, while the remainder is simply supported. Figure 2(b) shows the plate response at 191 Hz, obtained from a wave model with 96 wave functions, and illustrates the proper representation of the BC's.

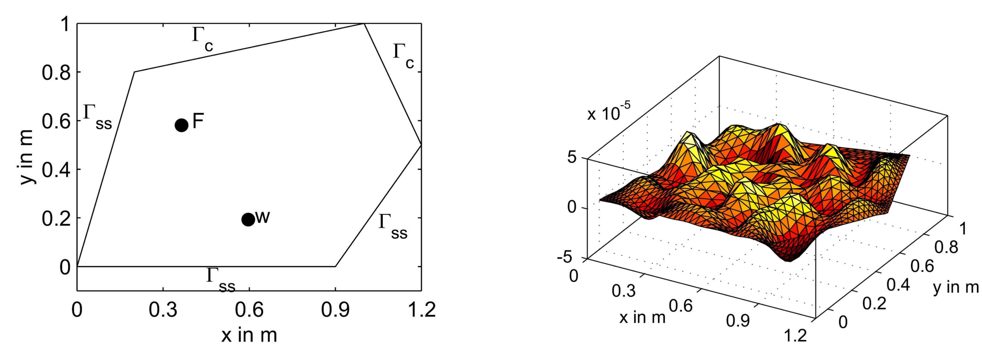

(a): Dimensions of convex plate. **(b):** Real part of plate deformation in m at 191 Hz.

Figure 2: Convex aluminum plate.

Several FE models are constructed using 8-noded quadratic plate elements. Table 1 lists the number of degrees of freedom in each model and indicates the prediction error at 191 Hz for the normal displacement at $\vec{r} = (0.60, 0.19)$ (see fig. 2(a)), relative to the result from a very large reference FE model. Table 1 lists also the CPU times, needed for solving the FE models at one frequency using MSC/NASTRAN and for both constructing and solving the wave model at one frequency using MATLAB. All calculations are performed on a HP-UX 9000/780 workstation. These results illustrate the enhanced convergence rate of the WB technique, in that it provides accurate prediction results with substantially smaller prediction models and smaller computational efforts than the FE method. In this way, the WB technique can be applied up to much higher frequencies, allowing accurate deterministic predictions for the mid-frequency range.

Model	# dof's	CPU time in s	relative error in %
FE 1	*7165*	*2.1*	
FE 2	*15785*	*5.9*	*17.0*
FE 3	*27765*	*12.7*	*3.4*
FE 4	*43105*	*23.3*	*reference*
WB	*96*	*2.4*	*4.7*

Table 1: Convergence results.

ACKNOWLEDGEMENTS

The research of B. van Hal is financed by a scholarship of the Institute for the Promotion of Innovation by Science and Technology in Flanders (IWT, Belgium). W. Desmet is a Postdoctoral Fellow of the Fund for Scientific Research - Flanders (FWO, Belgium).

REFERENCES

1. **W. Desmet**, *A wave based prediction technique for coupled vibro-acoustic analysis*, PhD Thesis, K.U.Leuven, division PMA, pp. 448pp.1998

2. **E. Trefftz**, Ein Gegenstuck zum Ritzschen Verfahren, In *Second Int. Cong. Appl. Mech.*, pp. 131-137, 1926